Chemical Engineering Journal 230 (2013) 166–171

Contents lists available at SciVerse ScienceDirect

Chemical Engineering Journal

journal homepage: www.elsevier.com/locate/cej

Preparation of nanoscale zero-valent iron supported on chelating resin with nitrogen donor atoms for simultaneous reduction of Pb^{2+} and NO_3^-

Jialu Shi, Shengnan Yi, Honglei He, Chao Long *, Aimin Li

State Key Laboratory of Pollution Control and Resource Reuse, School of the Environment, Nanjing University, 163 Xianlin Avenue, Nanjing 210023, China

HIGHLIGHTS

- Chelate resin DOW 3N was used as supporter of nanoscale Fe^0 for the first time.
- Nanoscale Fe^0 particles were well dispersed with the grain size of 10–30 nm.
- NZVI-DOW 3N can remove cation and anion contaminants simultaneously.

ARTICLE INFO

Article history:
Received 15 April 2013
Received in revised form 19 June 2013
Accepted 22 June 2013
Available online 1 July 2013

Keywords:
Donnan membrane effect
Chelating resin
Zero-valent iron
Nitrate
Lead

ABSTRACT

Polymeric ion exchanger has been proven to be an excellent carrier for metal nanoparticles due to chemical stability and robust mechanical strength. However, polymeric ion exchanger containing non-diffusible negatively or positively charged groups can only permit cation or anion contaminants to permeate into the polymer phase due to Donnan exclusion effect. In this study, zero-valent iron nanoparticles (NZVI) were immobilized within a chelating resin DOW 3N with pyridine functional groups through $NaBH_4$ reduction. TEM indicated that Fe^0 particles were clearly discrete and well dispersed on the surface of DOW 3N with grain size ranging from 10 to 30 nm. The reduction ability of NZVI-DOW 3N for Pb^{2+}, NO_3^- and their mixture were evaluated, respectively. The results showed that NO_3^- and Pb^{2+} can be reduced efficiently. In a binary solution, the removal efficiencies of NO_3^- and Pb^{2+} can reach 87% and 97%, respectively.

1. Introduction

Due to excess use of fertilizers and pesticides in agriculture and increased industrial activities, the groundwater and surface water are at a serious risk of pollution in most countries of the world. Nitrate is possibly the most widespread groundwater contaminant in the world, imposing a serious threat to drinking water supplies [1]. Excess NO_3^- in drinking water can cause adverse health effects, such as induction of "blue-baby syndrome" (methemoglobinemia), especially in infants, and the potential formation of carcinogenic nitrosamines. Heavy metals are highly reactive, bioaccumulative and extremely toxic elements above threshold concentrations. Toxic heavy metals in water are a growing threat to humanity [2]. Some studies have shown the co-existence of nitrate and heavy metal in natural water sources [3–5]. The co-existence of multiple contaminants makes water utilities facing increased challenges in providing safe drinking water.

Nanoscale zero valent iron (NZVI) has been extensively investigated for removal of a variety of pollutants and can provide greater reaction activity than conventional microscale materials. It has been demonstrated that NZVI can efficiently reduce anion contamination such as ClO_4^-, NO_3^- and heavy metals including Pb^{2+} and Ni^{2+} [6–9]. However, there are some potential limitations during application of NZVI. NZVI particles are prone to agglomerate into larger ones due to the tendency to reduce the high surface energies and intrinsic magnetic interaction [10], resulting in an adverse effect on both effective surface area and reduction performance; and moreover, the release or escape of nanoparticles into the environment can result in nanotoxicity [11]. To overcome the aforementioned drawbacks, an effective strategy is to stabilize NZVI within supporting materials, such as activated carbon [12,13], zeolite [14,15], porous silica [10,16], clay mineral [17] and polymeric resin [18–20].

Polymeric exchange resin has been proven to be an excellent carrier for metal and metal oxide nanoparticles due to chemical stability and robust mechanical strength [21]. Kim et al. [22] successfully immobilized ZVI on a cationic exchange membrane for dechlorination of trichloroethylene. Li et al. [18] immobilized NZVI particles on a cation exchange resin, and NZVI-resin composite was found to be highly effective in reductively debrominating decabromodiphenyl ether at ambient conditions. Shu et al. entrapped NZVI

---

* Corresponding author. Tel.: +86 25 89680380.
E-mail address: clong@nju.edu.cn (C. Long).

1385-8947/$ - see front matter © 2013 Elsevier B.V. All rights reserved.
http://dx.doi.org/10.1016/j.cej.2013.06.088

in cation exchange resin and observed successfully decoloration of acid blue 113 azo dye solution using NZVI-resin [23]. In addition to cation exchange resin, anion exchange resin was also used as a carrier for preparing metal and metal oxide nanoparticles [19,24]. Yang et al. immobilized Pd/Fe bimetallic nanoparticles within an anion exchanger resin D201 for dechlorination of monochlorobenzene, and monochlorobenzene was dechlorinated effectively to benzene [25].

Although polymer ion exchanger resin is an excellent carrier for NZVI, both cation exchanger and anion exchanger can only be available for limited contaminates due to Donnan co-ion exclusion effect [26,27]. The anion such as NO_3^-, ClO_4^- and AsO_4^{3-} are excluded from entering in the exchange phase of polymeric cation exchanger containing non-diffusible anion groups. Similar to polymeric cation exchanger, a high concentration of positively charged non-diffusible groups in an anion exchanger disallow permeation of cation contaminates such as Pb^{2+} and Cu^{2+}. It is well-recognized that the cation and anion contaminates usually exist in the aqueous solution simultaneously. Therefore, when NZVI supported on cation or anion exchange resin was used to treat wastewater contaminated cation and anion compounds simultaneously, only anion or cation contaminants can be reduced due to Donnan exclusion effect.

In this study, DOW 3N (DOWEX™ M4195), which is composed of a polystyrene cross-linked with divinyl benzene backbone and bis(2-pyridylmethyl)amine functional groups, was chosen as a supporting material for NZVI. The characterization of the NZVI-DOW 3N was obtained by Fourier transform infrared (FT-IR), X-ray photoelectron spectroscopy (XPS), transmission electron microscope (TEM), scanning electron microscopy (SEM), and BET-N_2 adsorption technique. NO_3^- and Pb^{2+} were selected as model compounds to examine the reduction ability of NZVI supported on DOW 3N. The use of polymers containing pyridine groups for supporting NZVI confers the following advantages: (1) the uncharged functional groups of pyridine allow the anion and cation contaminants to enter polymer phase; (2) Fe^{3+} can be strongly chelated through pyridine groups containing N as donor atoms [28,29], therefore, the high content of NZVI immobilized can be attained; (3) the release of iron ions into water can be avoided or alleviated due to the strong chelating properties of its functional groups. To the best of my knowledge, this is the first attempt to use DOW 3N immobilizing NZVI for simultaneous removal of inorganic anion and heavy metal.

2. Experimental

2.1. Materials

DOW 3N (DOWEX™ M4195) was purchased from Sigma Aldrich. Cation and anion exchange resin (D001 and D201) were supplied by Zhengguang Industrial Co., Ltd., China. Prior to use, the resins were extracted with ethanol for 8 h in a Soxlet apparatus, and washed by hydrochloric acid and sodium hydroxide. Their structure information is listed in Table 1. All chemicals including iron (III) chloride hexahydrate ($FeCl_3{\cdot}6H_2O$), sodium borohydride ($NaBH_4$), sodium nitrate ($NaNO_3$), lead (II) chloride ($PbCl_2$) and lead (II) nitrate ($Pb(NO_3)_2$) were analytical grade and used without further purification. All the solutions were prepared using ultrapure water produced by a Millipore-Q system (Millipore Synergy).

2.2. Preparation and characterization of NZVI resins

First, 0.5 g DOW 3N and D001 were added into 250 mL ethanol–water (V:V = 9:1) solution containing 3 g/L Fe^{3+}, respectively. For D201, 0.5 g polymer beads were added into 250 mL $FeCl_3{\cdot}6H_2O$ hydrochloric acid-water (V:V = 1:1) solution with 3 g/L Fe^{3+}. They were rotated for 24 h at 30 °C. Then all the resins were rinsed several times with ethanol and added into $NaBH_4$ solution (2% in mass), stirring by a blender under a N_2 atmosphere for 2 h at 20 °C. Finally, the resulting black beads were vacuum dried before characterization and batch experiments. The products were named as NZVI-DOW 3N, NZVI-D201, NZVI-D001, respectively.

The morphology of NZVI-DOW 3N was viewed with a scanning electron microscopy (Hitachi-3400N). The high-resolution transmission electron microscope (HR-TEM) image was taken on a JEM-2100. X-ray photoelectron spectroscopy (XPS) was performed to analyze the surface chemistry of NZVI using a PHI5000 VersaProbe. The specific surface areas and the pore size distribution were measured using an ASAP 2010 (Micromeritics Instrument Co., USA). The Fourier transform infrared spectroscopy (FT-IR) was recorded using a NEXUS870 FTIR Spectrometer. The amount of Fe loaded onto the polymeric hosts was determined by an atomic absorption spectrophotometer (AA-6300C) after being extracted by sulfuric acid solution (10 wt.%).

2.3. Experiments for chemical reduction

In the single solution, 44 mg/L nitrate and 100 mg/L Pb^{2+} were prepared using $NaNO_3$ and $PbCl_2$, respectively. In order to avoid the introduction of other ions, $Pb(NO_3)_2$ was used to prepare binary solution of NO_3^- and Pb^{2+}, and the concentration of Pb^{2+} and NO_3^- in binary solution was 103.5 mg/L and 62 mg/L, respectively. The pH of the solution was adjusted using 0.1 mol/L hydrochloric acid.

All the batch experiments were carried out in three-neck flacks placed in water bath incubator at 25 °C. Typically, NZVI-resin composites were mixed with 500 mL solution deoxygenated by N_2 and stirred with a mechanical stirrer. In order to keep an identical amount of NZVI in the solution (0.36 g NZVI/L), different doses of three kinds of NZVI-resin were added. At specific time interval,

Table 1
The physicochemical properties of hybrid NZVIs and host polymers.

Properties	DOW 3N	NZVI-DOW 3N	D201	NZVI-D201	D001	NZVI-D001
Matrix	Styrene-DVB		Styrene-DVB		Styrene-DVB	
Surface functional group	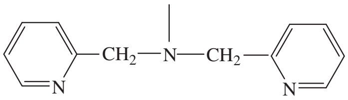		$-CH_2-N^+(CH_3)_3$		$-CH_2-SO_3H$	
BET surface area (m^2/g)	17.69	27.91	25.08	31.57	27.91	28.03
Average pore diameter (nm)	10.38	9.57	12.22	9.04	13.34	13.01
Pore volume (cm^2/g)	0.13	0.12	0.26	0.10	0.18	0.14
ZVI content (in Fe mass mg/g)	0	90.10	0	136.11	0	103.69

an aliquot of supernatant was sampled with a syringe and taken periodically to analyze.

Nitrate and nitrite in solution were determined by ion chromatography (Dionex 1000) with a column of IonPac AS11-HC (4 mm × 250 mm). Ammonia was analyzed by a UV–Vis spectrophotometer 2450 with the light absorption at 697 nm. The concentration of Pb^{2+} was determined by an atomic absorption spectrophotometer (AA-6300C, Japan).

3. Results and discussion

3.1. Characterization of NZVI-resin

Some important physicochemical properties of the solid samples employed in the study are shown in Table 1. The iron content in NZVI-DOW 3N was measured to be 90.10 mg/g. Compare with host polymer, NZVI loading resulted in an increase of BET surface area and a decrease in average pore diameter of NZVI-DOW 3N, the BET surface areas increased from 17.69 m^2/g to 27.91 m^2/g and the average pore diameter decreased from 10.38 nm to 9.57 nm. The variety of pore size after NZVI loading on DOW 3N could be observed clearly in Fig. S1 (Supplementary Material). In comparison with DOW 3N, an obvious increment of the pore volume was observed in the range of 2–30 nm pore diameter for NZVI-DOW 3N due to ZVI loadings. The loaded NZVI particles would block some inner pores or make the pores narrower. On the other side, they could provide more accessible surface and thereby increased the BET surface area.

It is learned from SEM and EDX images of DOW 3N and NZVI-DOW 3N (Fig. 1) that NZVI-DOW 3N exhibited a typical porous structure. This result suggests that the NZVI was uniformly immobilized into DOW 3N. In comparison with DOW 3N, more abundant pore structure was observed in the surface of NZVI-DOW 3N, which had been confirmed by the value of specific surface area. EDX analysis shows that the content of Fe was 1.08%, which was lower than 9.10% analyzed using atomic absorption spectrometer. The different Fe content showed that Fe^0 particles were mainly distributed in the inner pore surface of polymer bead, and that little of them were on the external surface of polymer.

TEM images of NZVI-DOW 3N (Fig. 2) indicates that the iron nanoparticles were clearly discrete and well dispersed on the

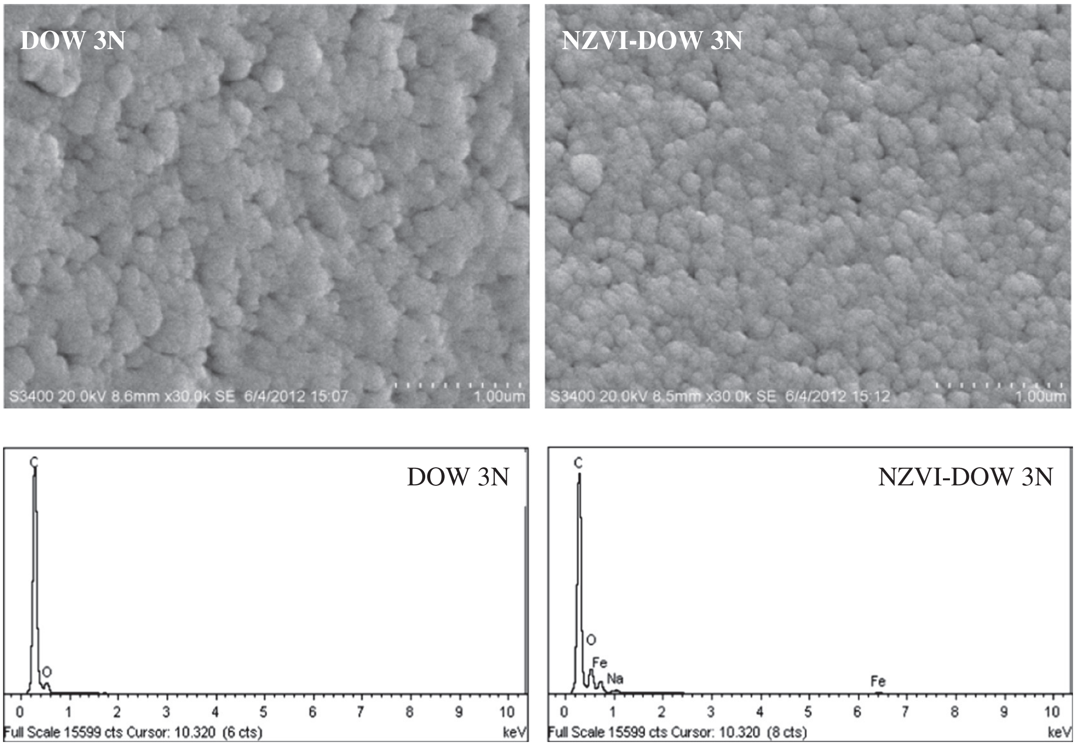

Fig. 1. SEM and EDX images of DOW 3N and NZVI-DOW 3N.

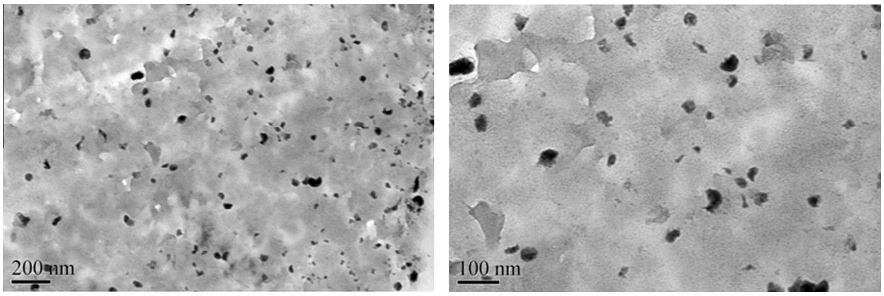

Fig. 2. TEM images of NZVI-DOW 3N.

surface of DOW 3N, without aggregation. Those particles are close to spherical with grain size ranging from 10 to 30 nm.

XPS technique was employed to analyze the oxidation state of the iron supported on the surface of DOW 3N. Fig. 3 shows XPS Fe 2p spectra of NZVI-DOW 3N. The photoelectron peaks at 705.96 eV and 718.92 eV represented the binding energies of Fe($2p_{3/2}$) and Fe($2p_{1/2}$) of zero-valent iron, respectively. The binding energies of Fe($2p_{3/2}$) = 709.84 eV and Fe($2p_{1/2}$) = 723.42 eV were assigned to the oxidized iron [30]. It suggested that the surface of NZVI consisted mainly of a layer of oxide film which might form during the vacuum drying process

The FTIR spectra of DOW 3N and NZVI-DOW 3N are shown in Fig. 4. The FTIR spectrum of DOW 3N showed four bands at 1589 cm^{-1}, 1569 cm^{-1}, 1433 cm^{-1} and 760 cm^{-1} which can be assigned to 2-picolylamine. All of these bands of DOW 3N were shifted to higher wave number values (1590 cm^{-1}, 1570 cm^{-1}, 1434 cm^{-1}, 762 cm^{-1}, respectively) in the spectrum of NZVI-DOW 3N. The shifts may be due to the coordinative bond between DOW 3N and iron [31]. The new absorption peak at 470 cm^{-1} in the spectrum of NZVI-DOW 3N corresponding to Fe–O stretches was observed [32]. These results can demonstrate that NZVI had been successfully loaded onto DOW 3N and the surface of the NZVI was partially oxidized, which were consistent with the results obtained from XPS. The other new absorption peaks at 2200–2400 cm^{-1} and 3209 cm^{-1} in the spectrum of NZVI-DOW 3N could be attributed to the bending vibration of B–O which was the residual after the reduction of iron using $NaBH_4$ (Fig. 4).

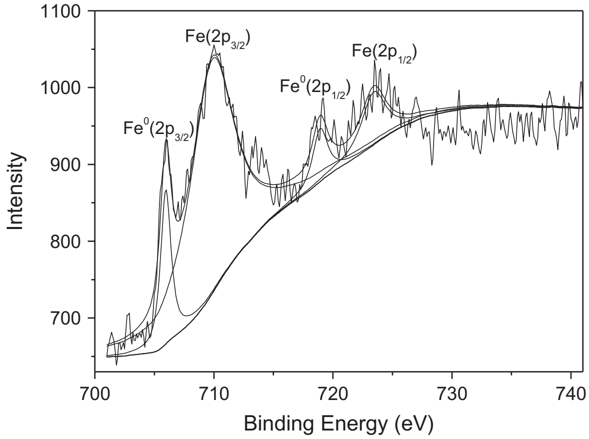

Fig. 3. XPS Fe 2p spectra of NZVI-DOW 3N.

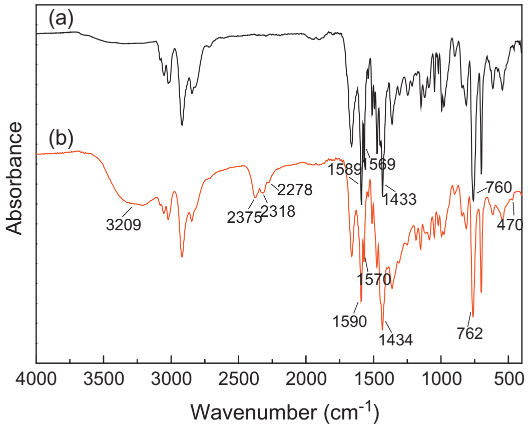

Fig. 4. The FTIR spectra of sample. (a) DOW 3N and (b) NZVI-DOW 3N.

3.2. Effect of Donnan membrane on removal of Pb^{2+} and NO_3^-

Fig. 5 shows comparison of Pb^{2+} and NO_3^- removal efficiency by NZVI supported on three different supporters at different pH values. It can be clearly seen that nanoscale zero-valent iron supported cation or anion exchange resin showed poor reduction capacities for anion contaminants (NO_3^-) or cation contaminant (Pb^{2+}), respectively, while NZVI-DOW 3N can efficiently remove both Pb^{2+} and NO_3^-. This phenomenon can result from different surface chemistry properties of three supporters. In a polymeric cation exchange resin (D001), negatively charged sulfonic acid groups are covalently attached to the polymer chains, and thus, they cannot permeate out of the polymer phase. Conversely, a polymeric anion exchange resin (D201) contains a high concentration of non-diffusible positively charged quaternary ammonium functional groups. Therefore, the high concentration of non-diffusible negatively or positively charged functional groups within D001 and D201 will prevent anion or cation contaminants from permeating into the polymer phase due to Donnan exclusion effect [26,27]. Due to non-existence of charged functional groups fixed on matrix of DOW 3N, NO_3^- and Pb^{2+} can permeate into the polymer phase of DOW 3N by diffusion.

Fig. 6 provides a schematic illustration of the difference among cation and anion exchanger and polymers containing pyridine groups as support materials. The presence of high concentration of non-diffusing fixed charges ($N(CH_3)_3^+$ or SO_3^-) in the polymer phase exhibits a net positive or negative charge in the surface of the polymer phase, which acts as a highly impermeable interface for Pb^{2+} or NO_3^-. Donnan exclusion effect will inhibit the diffusion of cationic or anionic contaminants [26,27], so Pb^{2+} or NO_3^- could be only reduced on the external surface of ion exchanger and the reduction capacity of nanoparticles loaded on exchanger will not be fully attained. But DOW 3N contains only uncharged bis(2-pyridylmethyl)amine functional groups, therefore, anion (NO_3^-) and cation (Pb^{2+}) can successfully permeate into the polymer phase without Donnan exclusion effect and be reduced by NZVI effectively (Fig. 6).

3.3. Reduction properties of NZVI-DOW 3N

3.3.1. Removal of anion contaminant (NO_3^-)

The efficiency on nitrate removal by NZVI-DOW 3N and DOW 3N was investigated and shown in Fig. 7. As can be seen in Fig. 7 and 94% of nitrate removed by NZVI-DOW 3N was obtained within 480 min and much higher than 30% removal by DOW 3N due to the adsorption. This result shows that NZVI-DOW 3N had the high reduction efficiency for nitrate. Also, ammonium and nitrite were detected in the aqueous solution, affirming that NO_3^- could be reduced at near neutral pH.

The reduction reaction of aqueous nitrate is a rather complicated one with possible intermediates and products, including NO_2, NO_2^-, NO, N_2O, N_2, NH_2OH, N_2H_4, and NH_3/NH_4^+. In this study, the mass balance of total nitrogen species was calculated after the reduction reaction was carried out for 480 min. As a result, the overall amount of nitrogen species decreased 18% compared with the initial amount, the decreased amount of nitrogen species in the solution is probably due to the formation of ammonia gas or/and nitrogen gas, or the adsorption of NO_3^- and NO_2^- by the supporter, iron oxide and hydroxides which was formed during the reduction reaction.

3.3.2. Removal of cation contaminant (Pb^{2+})

The removal of Pb^{2+} from the aqueous solution with NZVI-DOW 3N and DOW 3N was shown in Fig. 8. The equilibrium for Pb^{2+} removal from solution was reached within the first 90 min using NZVI-DOW 3N and 5 min using DOW 3N in the absence of NZVI.

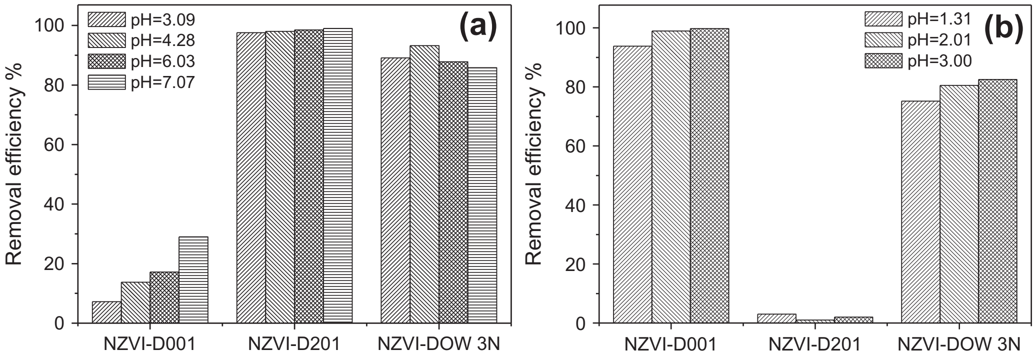

Fig. 5. The removal efficiency of NO_3^- (a) and Pb^{2+} (b) by nanoscale zero-valent iron supported on D001, D201 and DOW 3N at different pH values.

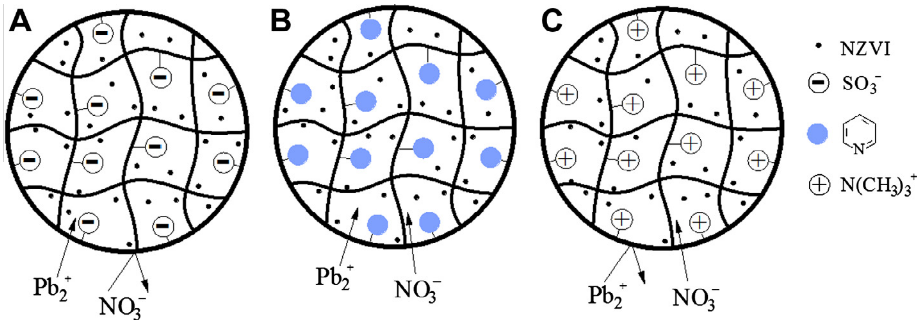

Fig. 6. Schematic illustrating: permeation of anion and cation contaminant into the polymer phase in the presence of (A) non-diffusible anions (cation exchanger), (B) uncharged functional groups and (C) non-diffusible cations (anion exchanger).

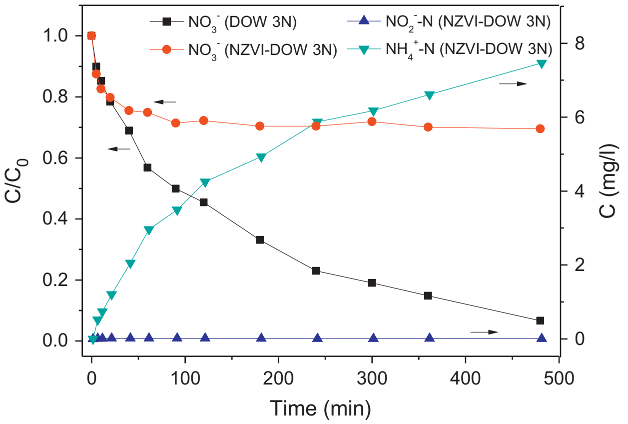

Fig. 7. The removal kinetics of nitrate by DOW 3N and NZVI-DOW 3N.

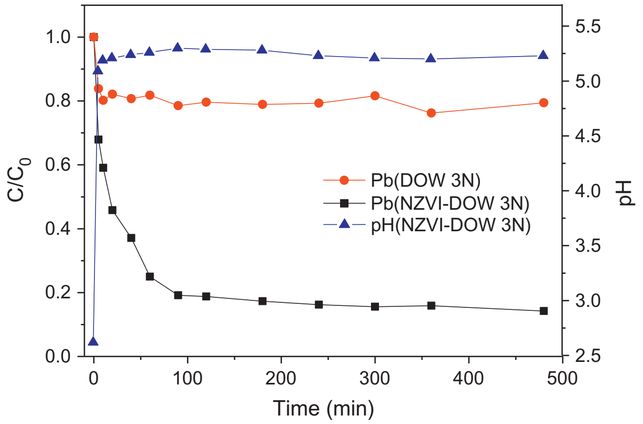

Fig. 8. The removal kinetics of Pb^{2+} by DOW 3N and NZVI-DOW 3N.

However, 85.79% removal of Pb^{2+} from solution can be obtained using NZVI-DOW 3N, while only 20.54% removal of Pb^{2+} using DOW 3N. The pH of the solution varied from 2.62 to 5.23 for removal of Pb^{2+} by NZVI-DOW 3N, indicating that lead oxides and lead hydrates did not form during the removal of Pb^{2+} [33]. Therefore, it can be concluded that Pb^{2+} removal from solution was mainly reduced to Pb^0; Pb^{2+} was first absorbed onto DOW 3N by chelating with pyridine groups containing N as donor atoms, and then further reduced by NZVI.

3.3.3. *Removal of* NO_3^- *and* Pb^{2+} *in binary solution by NZVI-DOW 3N*

In order to better understand the reduction properties of NZVI-DOW 3N, reduction of NO_3^- and Pb^{2+} in binary solution with initial pH 5.33 by NZVI-DOW 3N was investigated. From the Fig. 9, it is clearly learned that NZVI-DOW 3N showed high simultaneous removal efficiency for Pb^{2+} and NO_3^-. Above 87% of nitrate was removed and was mainly reduced to ammonium, affirming that NO_3^- could be reduced at near neutral pH by NZVI-DOW 3N. Ammonium accounts for about 98% of the reaction products and the overall amount of nitrogen species was nearly equal to the initial amount. However, the removal efficiency of NO_3^- was about 94% without the presence of Pb^{2+}. The decrease of the removal efficiency for NO_3^- in binary solution was because that Pb^{2+} may occupy the available active sites, thereby lowering the NO_3^- removal efficiency.

The removal efficiency of Pb^{2+} was as high as 97%. It is found that pH of the solution increased from 5.33 to 8.92 during the reduction reaction of NO_3^- and Pb^{2+}. The high pH may led to the transformation of Pb^{2+} into lead oxides and lead hydrates on the surface of NZVI-DOW 3N, enhancing the removal efficiency of Pb^{2+}. Therefore, if NO_3^- was existed in the solution, it can further

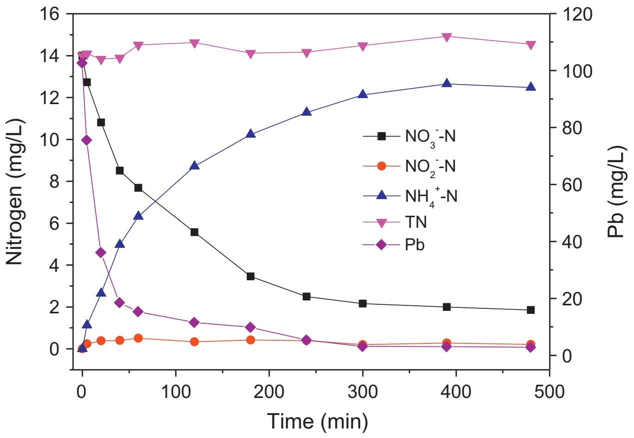

Fig. 9. The removal kinetics of NO_3^- and Pb^{2+} in binary solution by NZVI-DOW 3N.

strengthen the removal efficiency of Pb^{2+} by increasing the solution pH.

On the basis of the above results, it is possible for NZVI-DOW 3N to offer great potential in treating wastewater contaminated cation and anion compounds simultaneously.

4. Conclusions

In this study, nanozero valent iron was successfully immobilized into DOW 3N containing bis(2-pyridylmethyl)amine functional groups. EDX, XPS and FT-IR spectroscopy confirmed the formation of NZVI in the polymeric resin. The results obtained from SEM indicated that NZVI loaded onto DOW 3N was well dispersed with diameter ranging from 10 to 30 nm. NZVI loadings resulted in a significant increase in BET surface area from 17.69 m^2/g to 27.91 m^2/g.

Due to non-existence of Donnan exclusion effect, both NO_3^- and Pb^{2+} can diffuse into the polymer phase of DOW 3N. Therefore, NZVI-DOW 3N composite showed a high efficiency for removing NO_3^- and Pb^{2+} from aqueous solution simultaneously. The removal efficiency for Pb^{2+} and NO_3^- were 97% and 87% in binary solution, respectively.

Acknowledgements

This research was financially funded by Program for New Century Excellent Talents in University (Grant No. NCET-11-0230), Qing Lan Project of Jiangsu Province, and Program for Changjiang Scholars Innovative Research Team in University. This research was also sponsored by Major Special Project of Water Pollution Control and Management Technology of PR China (Grant No. 2012ZX07101-003).

Appendix A. Supplementary material

Supplementary data associated with this article can be found, in the online version, at http://dx.doi.org/10.1016/j.cej.2013.06.088.

References

[1] L.J. Puckett, Identifying the major sources of nutrient water-pollution, Environ. Sci. Technol. 29 (1995) A408–A414.

[2] S.H. Hasan, P. Srivastava, M. Talat, Biosorption of Pb(II) from water using biomass of Aeromonas hydrophila: central composite design for optimization of process variables, J. Hazard. Mater. 168 (2009) 1155–1162.

[3] T.E. Keskin, Nitrate and heavy metal pollution resulting from agricultural activity: a case study from Eskipazar (Karabuk, Turkey), Environ. Earth Sci. 61 (2010) 703–721.

[4] Z.-W. Hao, X.-H. Xu, J. Jin, P. He, Y. Liu, D.-H. Wang, Simultaneous removal of nitrate and heavy metals by iron metal, J. Zhejiang Univ-SC B 6 (2005) 307–310.

[5] Y. Zhang, F. Zhong, S. Xia, X. Wang, Ieee, Effect of initial nitrate concentrations and heavy metals on autohydrogenotrohic denitrification, 3rd iCBBE, 1–11 (2009) 5637–5640.

[6] J.S. Cao, D. Elliott, W.X. Zhang, Perchlorate reduction by nanoscale iron particles, J. Nanopart. Res. 7 (2005) 499–506.

[7] Y.-H. Hwang, D.-G. Kim, H.-S. Shin, Mechanism study of nitrate reduction by nanozero valent iron, J. Hazard. Mater. 185 (2011) 1513–1521.

[8] X. Zhang, S. Lin, X.Q. Lu, Z.L. Chen, Removal of Pb(II) from water using synthesized kaolin supported nanoscale zero-valent iron, Chem. Eng. J. 163 (2010) 243–248.

[9] X.Q. Li, W.X. Zhang, Iron nanoparticles: the core-shell structure and unique properties for Ni(II) sequestration, Langmuir 22 (2006) 4638–4642.

[10] T. Phenrat, N. Saleh, K. Sirk, R.D. Tilton, G.V. Lowry, Aggregation and sedimentation of aqueous nanoscale zerovalent iron dispersions, Environ. Sci. Technol. 41 (2006) 284–290.

[11] G. Oberdorster, E. Oberdorster, J. Oberdorster, Nanotoxicology: an emerging discipline evolving from studies of ultrafine particles, Environ. Health Persp. 113 (2005) 823–839.

[12] H.J. Zhu, Y.F. Jia, X. Wu, H. Wang, Removal of arsenic from water by supported nanozero-valent iron on activated carbon, J. Hazard. Mater. 172 (2009) 1591–1596.

[13] H. Choi, S.R. Al-Abed, Effect of reaction environments on the reactivity of PCB (2-chlorobiphenyl) over activated carbon impregnated with palladized iron, J. Hazard. Mater. 179 (2010) 869–874.

[14] S. Lee, K. Lee, S. Rhee, J. Park, Development of a new zero-valent iron zeolite material to reduce nitrate without ammonium release, J. Environ. Eng-asce 133 (2007) 6–12.

[15] W. Wang, M.H. Zhou, Q.O. Mao, J.J. Yue, X. Wang, Novel NaY zeolite-supported nanoscale zero-valent iron as an efficient heterogeneous Fenton catalyst, Catal. Commun. 11 (2010) 937–941.

[16] T.H. Zheng, J.J. Zhan, J.B. He, C. Day, Y.F. Lu, G.L. McPherson, G. Piringer, V.T. John, Reactivity characteristics of nanoscale zerovalent iron–silica composites for trichloroethylene remediation, Environ. Sci. Technol. 42 (2008) 4494–4499.

[17] Y. Zhang, Y. Li, J. Li, L. Hu, X. Zheng, Enhanced removal of nitrate by a novel composite: nanoscale zero valent iron supported on pillared clay, Chem. Eng. J. 171 (2011) 526–531.

[18] A. Li, C. Tai, Z.S. Zhao, Y.W. Wang, Q.H. Zhang, G.B. Jiang, J.T. Hu, Debromination of decabrominated diphenyl ether by resin-bound iron nanoparticles, Environ. Sci. Technol. 41 (2007) 6841–6846.

[19] Z. Jiang, L. Lv, W. Zhang, Q. Du, B. Pan, L. Yang, Q. Zhang, Nitrate reduction using nanosized zero-valent iron supported by polystyrene resins: role of surface functional groups, Water Res. 45 (2011) 2191–2198.

[20] C.J. Lin, Y.H. Liou, S.L. Lo, Supported Pd/Sn bimetallic nanoparticles for reductive dechlorination of aqueous trichloroethylene, Chemosphere 74 (2009) 314–319.

[21] P. Puttamraju, A.K. SenGupta, Evidence of tunable on-off sorption behaviors of metal oxide nanoparticles: role of ion exchanger support, Ind. Eng. Chem. Res. 45 (2006) 7737–7742.

[22] H. Kim, H.J. Hong, Y.J. Lee, H.J. Shin, J.W. Yang, Degradation of trichloroethylene by zero-valent iron immobilized in cationic exchange membrane, Desalination 223 (2008) 212–220.

[23] H.Y. Shu, M.C. Chang, C.C. Chen, P.E. Chen, Using resin supported nanozero-valent iron particles for decoloration of Acid Blue 113 azo dye solution, J. Hazard. Mater. 184 (2010) 499–505.

[24] S. Sarkar, L.M. Blaney, A. Gupta, D. Ghosh, A.K. SenGupta, Use of ArsenX(np), a hybrid anion exchanger, for arsenic removal in remote villages in the Indian subcontinent, React. Funct. Polym. 67 (2007) 1599–1611.

[25] L. Yang, L. Lv, S.J. Zhang, B.C. Pan, W.M. Zhang, Catalytic dechlorination of monochlorobenzene by Pd/Fe nanoparticles immobilized within a polymeric anion exchanger, Chem. Eng. J. 178 (2011) 161–167.

[26] L. Cumbal, A.K. Sengupta, Arsenic removal using polymer-supported hydrated iron(III) oxide nanoparticles: role of Donnan membrane effect, Environ. Sci. Technol. 39 (2005) 6508–6515.

[27] S. Sarkar, A.K. Sengupta, P. Prakash, The donnan membrane principle: opportunities for sustainable engineered processes and materials, Environ. Sci. Technol. 44 (2010) 1161–1166.

[28] C.V. Diniz, V.S.T. Ciminelli, F.M. Doyle, The use of the chelating resin Dowex M-4195 in the adsorption of selected heavy metal ions from manganese solutions, Hydrometallurgy 78 (2005) 147–155.

[29] C.V. Diniz, F.M. Doyle, V.S.T. Ciminelli, Effect of pH on the adsorption of selected heavy metal ions from concentrated chloride solutions by the chelating resin Dowex M-4195, Sep. Sci. Technol. 37 (2002) 3169–3185.

[30] B.J. Tan, K.J. Klabunde, P.M.A. Sherwood, X-ray photoelectron-spectroscopy studies of solvated metal atom dispersed catalysts – monometallic iron and bimetallic iron cobal particles on alumina, Chem. Mater. 2 (1990) 186–191.

[31] K.H. Wu, Y.R. Wang, W.H. Hwu, FTIR and TGA studies of poly(4-vinylpyridine-co-divinylbenzene)-Cu(II) complex, Polym. Degrad. Stabil. 79 (2003) 195–200.

[32] X. Zhang, S. Lin, Z.L. Chen, M. Megharaj, R. Naidu, Kaolinite-supported nanoscale zero-valent iron for removal of Pb^{2+} from aqueous solution: reactivity, characterization and mechanism, Water Res. 45 (2011) 3481–3488.

[33] Y.-C. Lee, E.J. Kim, D.A. Ko, J.-W. Yang, Water-soluble organo-building blocks of aminoclay as a soil-flushing agent for heavy metal contaminated soil, J. Hazard. Mater. 196 (2011) 101–108.